Journal of Chromatography B, 1031 (2016) 146–153

Contents lists available at ScienceDirect

Journal of Chromatography B

journal homepage: www.elsevier.com/locate/chromb

Separation and analysis of mono-glucosylated lipids in brain and skin by hydrophilic interaction chromatography based on carbohydrate and lipid moiety

Kazuki Nakajima[a], Hisako Akiyama[a], Kaori Tanaka[a], Ayako Kohyama-Koganeya[a], Peter Greimel[b], Yoshio Hirabayashi (Ph.D.)[a,*]

[a] Molecular Membrane Neuroscience, RIKEN Brain Science Institute, RIKEN, 2-1 Hirosawa, Wako, Saitama 351-0198, Japan
[b] Lipid Biology Laboratory, RIKEN, 2-1 Hirosawa, Wako, Saitama 351-0198, Japan

ARTICLE INFO

Article history:
Received 18 April 2016
Received in revised form 23 July 2016
Accepted 26 July 2016
Available online 26 July 2016

Keywords:
Hydrophilic interaction chromatography
Zwitterionic phase
Mass spectrometry
Glucosylceramide
Phopsphatidylglucoside
Glucosylated lipid
Lipid isomer

ABSTRACT

Mono-glycosylated sphingolipids and glycerophospholipids play important roles in diverse biological processes and are linked to a variety of pathologies, such as Parkinson disease. The precise identification of the carbohydrate head group of these lipids is complicated by their isobaric nature and by substantial differences in concentration in different biological samples. To overcome these obstacles, we developed a zwitterionic (ZIC)-hydrophilic interaction chromatography (HILIC) electrospray ionization tandem mass spectrometry method. ZIC-HILIC preferentially retains inositol, followed by glucose- and galactose-featuring lipids. Comparison with unmodified silica gel HILIC stationary phase revealed different retention specificity. To evaluate the precision of ZIC-HILIC, we quantified glucosyl- (GlcCer) and galactosylceramides (GalCer) in seven different regions of the mouse brain and discovered that GlcCer and GalCer concentrations are inversely related. The highest GalCer (lowest GlcCer) content was found in the medulla oblongata and hippocampus, whereas the highest GlcCer (lowest GalCer) content was found in other regions. With a neutral loss scan, ZIC-HILIC resolved glucosylceramide species featuring non-hydroxylated fatty acid, hydroxylated fatty acid, and trihydroxy sphingoid bases in mouse epidermis samples. This demonstrates that our ZIC-HILIC-based approach is a valuable tool for characterizing the structural diversity of mono-glucosylated lipids in biological material and for quantifying these important lipids.

1. Introduction

Mono-glucosylated lipids, such as glucosylceramide (GlcCer), phosphatidylglucoside (PtdGlc), and cholesterylglucoside (ChlGlc), play important roles in various biological processes [1–3]. For example, GlcCer is a key intermediate in the synthesis of most glycosphingolipids, and it also acts as a glucose donor in ChlGlc biosynthesis [4]. In brain tissue, the glucose head group of GlcCer is predominantly replaced by its C4 epimer, galactose, giving rise to galactosylceramide (GalCer). GlcCer and GalCer are integral to neural function, performing different roles in the brain. GalCer is a component of myelin and plays a critical role in myelin-related functions [5], whereas GlcCer is involved in axonal growth [6,7]. On the other hand, PtdGlc, a novel glycerol-type glucosylated lipid, is a minor component of lipid rafts [8]. Recently, PtdGlc was found to serve as an important guidance cue for spinal cord sensory axons after it undergoes hydrolysis by phospholipases to lyso-PtdGlc [9]. However, phosphatidylinositol (PtdIns), the isobaric isomer of PtdGlc, is abundantly present in brain.

In non-neural tissues, GlcCer exhibits structural complexity, and each GlcCer species has distinctive functions, as in ceramide species [10]. In skin, acylated or hydroxylated GlcCer are involved in epidermal cell differentiation [11,12]. Consequently, a highly reproducible analytical method capable of isometric-based

Abbreviations: ChlGlc, cholesterylglucoside; CV, coefficients of variation; ESI–MS/MS, electrospray ionization tandem mass spectrometry; GalCer, galactosylceramide; GlcCer, glucosylceramide; HexCer, hexosylceramide; HILIC, hydrophilic interaction chromatography; HPTLC, high-performance thin-layer chromatography; LC, liquid chromatography; MRM, multiple reaction monitoring; non-OHFA, non-hydroxy fatty acid; αOHFA, alpha-hydroxy fatty acid; ωOHFA, omega-hydroxy fatty acid; HFA, hydroxy fatty acid; PtdGal, phosphatidylgalactoside; PtdGlc, phosphatidylglucoside; PtdIns, phosphatidylinositol; RSD, relative standard deviation; TLC, thin-layer chromatography; ZIC, zwitterionic; ZIC-HILIC, zwitterionic hydrophilic interaction chromatography.

* Corresponding author.
E-mail address: hirabaya@riken.jp (Y. Hirabayashi).

http://dx.doi.org/10.1016/j.jchromb.2016.07.047
1570-0232/

separation via the carbohydrate and ceramide moiety is highly desired in order to gain a better understanding of the biological functions of mono-glycosylated lipids.

Liquid chromatography (LC) electrospray ionization tandem mass spectrometry (ESI–MS/MS) is a powerful tool for lipidomic analyses. Further improvement is achieved via a two-dimensional LC setup, featuring a combination of two different chromatographic methods. This setup enhances identification of minor lipid species in qualitative analysis as well as reproducibility in quantitative analysis [13,14]. Reversed-phase chromatography is used widely to separate lipid samples, primarily based on the length and degree of saturation of their respective alkyl chains. Unfortunately, subtle alterations of the head group, such as substituting glucose for galactose, cannot be resolved [15]. By contrast, hydrophilic interaction chromatography (HILIC), a type of normal phase chromatography, is able to resolve lipids based on their head groups [16–18]. HILIC separation is based on the analyte partitioning between acetonitrile-rich mobile phase and a water-rich layer absorbed on the hydrophilic stationary phase. More hydrophilic analytes are retained on the column as their partitioning equilibrium shifts more toward the water layer on the stationary phase [19,20].

While the HILIC method was initially developed for the separation of amino acids, the successful separation of GlcCer from GalCer has also been reported using a fused-core silica and amino column [21,22]. More recently, a HILIC-based method using ultra-performance LC and supercritical fluid chromatography has been demonstrated to discriminate sufficiently between GlcCer and GalCer in brain tissue samples [23,24]. While these approaches have been used to quantify both GlcCer and GalCer, they suffer from substantial variability among different samples [21–24]. Consequently, an alternative method with improved resolution of complex GlcCer would be highly desirable.

A zwitterionic (ZIC) stationary phase consists of oppositely charged groups and is a phase that can be used to separate phospholipid classes based on electrostatic interactions [25]. In general, a ZIC stationary phase retains a thick hydration layer that generates strong hydrophilic interactions with analytes [20]. This feature facilitates the separation of configurational isomers and the discrimination of hydroxylated molecules, such as glycopeptides and carbohydrates [26–29].

In the present study, we evaluated the efficacy of ZIC-HILIC stationary phases for isometric separation of a variety of glucosylated lipid classes. Following method optimization, we first compared the chromatographic behaviors of two classes of glycolipids on a ZIC-HILIC with an unmodified silica gel HILIC stationary phase. Next, we evaluated the utility and reproducibility of our method for the quantitative analysis of GlcCer in brain tissue and demonstrated that it is highly suitable for analyzing other glycolipids, such as PtdGlc and PtdIns. Additionally, the successful discrimination of complex epidermal GlcCer mixtures based on their ceramide moieties via a two-column setup confirmed the suitability of our ZIC-HILIC method for characterizing the carbohydrate and ceramide moieties of GlcCer simultaneously.

2. Materials and methods

2.1. Materials

Lipid standards were purchased from Avanti Polar lipids (Andover, MA, USA). PtdGlc (18:0/20:0), PtdGlc (18:0/18:0), PtdGal (18:0/20:0), and acetylated-PtdGlc (18:0/20:0) were synthesized, as we reported previously [30,31]. Ammonium formate was purchased from Sigma Aldrich Japan (Tokyo, Japan). Acetonitrile and methanol were purchased from Thermo Fisher Scientific (Waltham, MA, USA). Chloroform and distilled water were purchased from Kanto Kagaku (Tokyo, Japan). The solvents were of HPLC grade. All other materials were either from WAKO (Osaka, Japan) or Sigma Aldrich Japan. All materials and solvents were used as supplied without further purification.

2.2. Lipid extraction

All animal experiments were performed in compliance with RIKEN institutional guidelines. Ten-week-old and 9-month-old C57BL/6J mice (Charles River Laboratories, Japan) were deeply anesthetized, and the cranium was carefully dissected open. The entire brain was removed and divided into seven parts based mostly on standard anatomical regions: olfactory bulb, hypothalamus, cerebellum, medulla oblongata, hippocampus, cortex, and other regions not included in the first six. Each separated region was immediately frozen in liquid nitrogen and stored until analysis. Mouse epidermal sheets were obtained according to previous reports [11,12].

Total lipids were extracted from lyophilized tissues added with GlcCer (d18:0/12:0) containing 5 pmol/mg of lyophilized tissue, according to the method of Bligh and Dyer [32]. The total lipid extracts were hydrolyzed in 2 ml of 0.1 M potassium hydroxide in chloroform/methanol (2:1, v/v) for 2 h at room temperature, neutralized with acetic acid [21], and partitioned according to the Folch method. The lower phase was collected and dried under a stream of nitrogen. Lipids from mouse epidermal sheets were precipitated in acetone (2 ml) for 2 h on ice and collected by centrifugation.

2.3. LC–MS/MS analysis

Samples were analyzed on a semi-micro LC system 100XL (Eksigent, Dublin, CA, USA) coupled to a triple quadrupole linear ion trap mass spectrometer, QTRAP4500 (SCIEX, Toronto, Canada).

2.3.1. Chromatographic conditions

Chromatographic conditions based on a previous report [18] were modified as described below. ZIC column with phosphocholine phase (ZIC-cHILIC, 2.1 mm i.d. × 150 mm, 3 μm; Merck SeQuant, Umea, Sweden); ZIC column with sulfobetaine phase (2.1 mm i.d. × 150 mm, 3.5 μm; Merck SeQuant); and Atlantes silica HILIC column (2.1 mm i.d. × 150 mm, 3 μm; Waters, MA, USA) were used as indicated and regenerated weekly with 30 column volumes of washing solution (acetonitrile/water, 80:20, v/v). ZIC columns with phosphocholine and sulfobetaine phase were equilibrated with mobile phase A (acetonitrile/water/formic acid, 96/3/1, v/v/v, with 5 mM ammonium formate) and the Atlantes silica HILIC column with an alternative mobile phase A (acetonitrile/methanol/formic acid, 97/2/1, v/v/v, with 5 mM ammonium formate), each at a flow rate of 150 μl/ml.

Samples were dissolved in chloroform/methanol (4/1, v/v), diluted 10-fold with mobile phase A, and a 10 μl aliquot was injected via an injector valve equipped with a 20 μl sample loop filled with acetonitrile. Upon injection, the chromatography gradient and data collection by the mass spectrometry was initiated. Lipids were eluted with the following gradient of mobile phase B (methanol/water/formic acid, 89/10/1, v/v/v, with 20 mM ammonium formate): 0% B over 3.3 min; 0–70% linear increase of B over 16.7 min; 70–100% linear gradient of B over 1 min; 100% washing with B for 5 min; and finally equilibrated with A for 20 min.

To allow comparison of the chromatographic behaviors between the employed HILIC columns, the retention factors (k) of phosphatidyl hexosides and PtdIns were calculated. The dead time ($t_0 = 3.33 \pm 0.4$) was determined with benzophenone (50 pmol) in three experiments.

2.3.2. ESI–MS/MS conditions

First, the optimal conditions for GlcCer (d18:1/12:0) and PtdGlc (18:0/20:0) were determined by adjusting the declustering potential, entrance potential, collision energy, and collision cell exit potential. Subsequently, the ionization conditions were optimized. Analysis of target lipids was conducted in the multiple reaction monitoring (MRM) mode using specific precursor-product ion pairs. The employed precursor ions (Q1), product ions (Q3), and collision energies are summarized in Table S1. PtdGlc was analyzed in the negative ion mode according to our previous report [33], using the following settings: ion spray voltage, −4500 V; curtain gas, 30 psi; temperature, 600 °C. GlcCer was analyzed in the positive ion mode with the following settings: ion spray voltage, 5000 V; curtain gas, 30 psi; temperature, 200 °C. The neutral-loss scan for hexosylceramide (HexCer)-specific detection was performed with the following settings according to our previous report [34]: neutral loss, 180 Da; scan range of the instrument, *m/z* 400–1000; scan speed, 2,000/s; collision energy, 30 eV.

Each peak was integrated using MultiQuant software and quantified based on the peak areas of each standard. GlcCer and GalCer content was normalized against the internal standard (GlcCer, d18:1/12:0) recovery and expressed as pmol/mg lyophilized tissues. The values represent the averages of three experiments.

2.4. High-performance thin-layer chromatography (HPTLC)

Lipid mixtures dissolved in chloroform/methanol (2:1, v/v) were separated on a boric acid coated HPTLC plate (silica gel 60; Merck Millipore, Germany), and developed in chloroform/methanol/2.5 M ammonia solution (65:35:8, v/v/v) [35]. Neutral glycosphingolipids were visualized by spraying orcinol reagent, followed by heating on a hot plate at 120 °C for 10 min. Identities of the stained lipids were ascertained by reference standards.

3. Results and discussion

3.1. Optimization and reproducibility

HILIC separation of lipids is usually achieved with mobile phases composed of 95–97% acetonitrile in water or a volatile solvent [16–19,21,22,25]. For example, bacterial phospholipids are separated on ZIC-HILIC with a mobile phase containing 5% water [25]. In the present study, we selected an acetonitrile/water mixture (96:4, v/v) containing 5 mM ammonium formate, which sufficiently retained GlcCer and PtdGlc samples on the column. In order to ensure reproducible results, the column was regenerated with acetonitrile/water (80:20, v/v) prior to each analysis.

The reproducibility of elution times and peak areas was confirmed by analyzing a synthetic mixture of PtdGlc (18:0/18:0) and PtdIns (18:0/18:0). Over seven runs, the results were highly reproducible (Fig. S1), with a retention time coefficients of variation (CV) for PtdGlc and PtdIns of ~0.9%. The peak area CVs of PtdGlc and PtdIns were 6.7% and 7.4%, respectively. This represents a significant improvement compared with our previously reported method based on normal phase chromatography with a chloroform-based solvent system [33], demonstrating the suitability of ZIC-HILIC to reliably quantify PtdGlc.

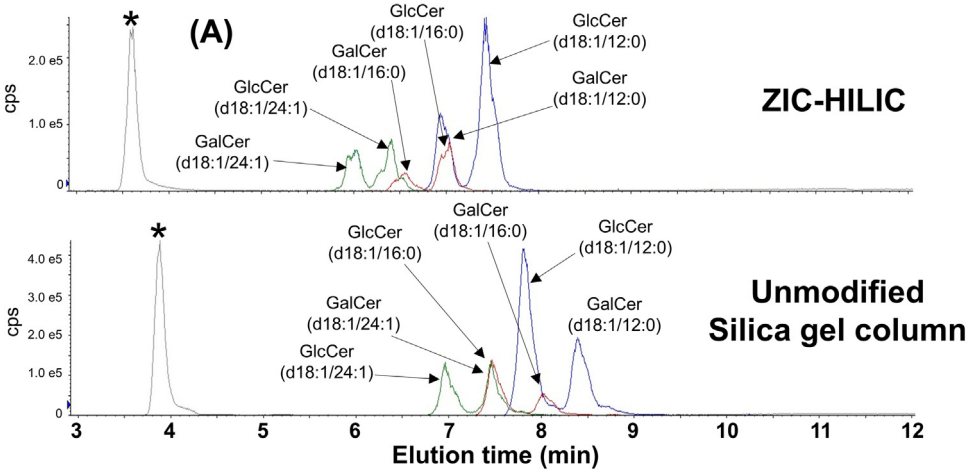

(B)

Lipids	Retention factor (*k*)	
	ZIC-HILIC	Unmodified silica gel
PtdGal (18:0/20:0)	3.36	3.00
PtdGlc (18:0/18:0)	3.41	2.92
PtdGlc *sn*=1.2 (18:0/20:0)	3.38	2.90
PtdGlc *sn*=2.3 (18:0/20:0)	3.39	2.91
6-O-acetyl PtdGlc (18:0/20:0)	3.16	2.67
PtdIns (18:0/20:4)	3.61	3.12
PtdIns (18:0/18:0)	3.64	3.18
Lyso PtdIns (18:0)	4.51	3.64
Lyso PtdGlc (18:0)	4.26	3.34

Fig. 1. Chromatographic behaviors of glucosylated lipids on a ZIC-HILIC column and on an unmodified silica gel column for comparison. (A) Mass chromatograms of standard reference material containing hexosylceramide (HexCer) with d18:1/24:1 (green), d18:1/16:0 (red), and d18:1/12:0 (blue). (B) Retention factors (*k*) of phosphatidyl hexosides and phosphatidylinositol (PtdIns) for dead time are indicated with asterisks.

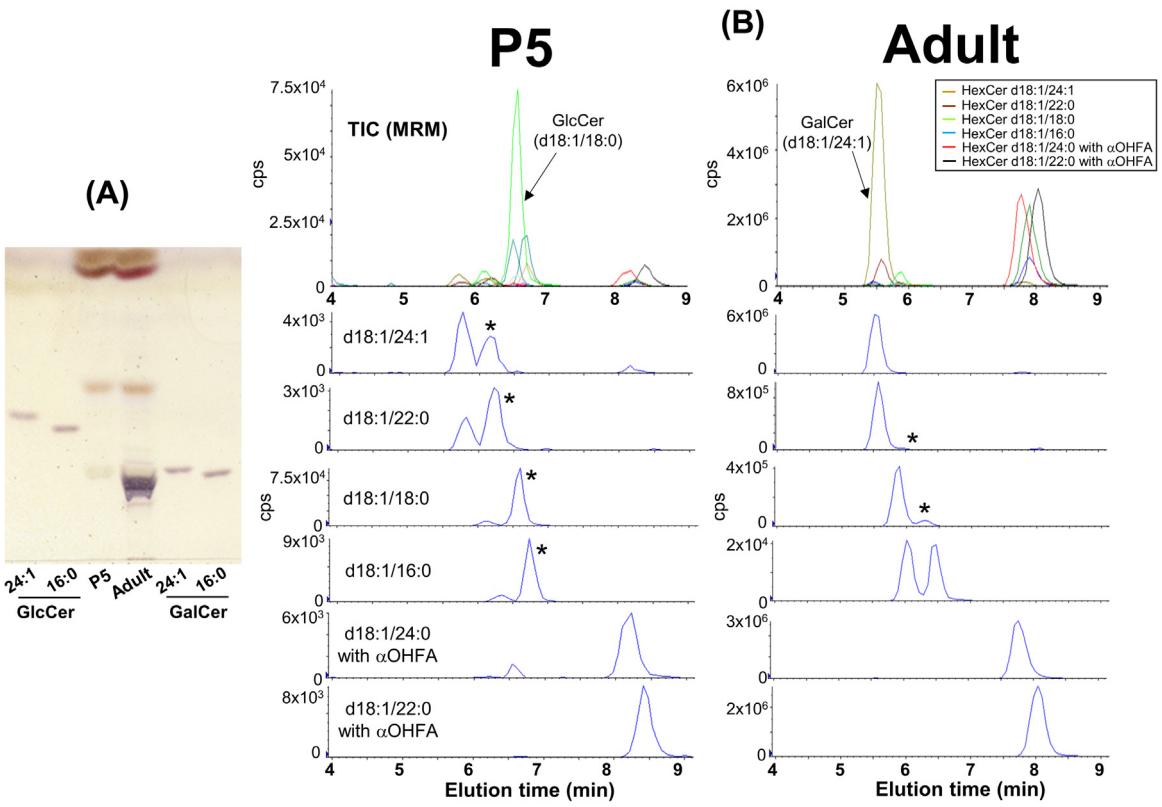

Fig. 2. Profiles of lipid mixtures extracted from mouse brains from postnatal day 5 (P5) and 10-week-old (adult) mice. (A) TLC profiles of both lipid mixtures and standard references of four types of HexCer by using a boric-acid-impregnated TLC plate. (B) Representative mass chromatograms of both lipid mixtures analyzed by ZIC-HILIC. Various glucosylceramide (GlcCer) species present in minute quantities in brain tissue (asterisk) were separated from galactosylceramide (GalCer) and quantified.

3.2. ZIC-HILIC versus unmodified silica gel HILIC

Next we compared the chromatographic behaviors of standard reference materials, such as HexCers, phosphatidyl hexosides, and PtdIns (Fig. 1), on an unmodified silica gel HILIC with ZIC-HILIC. The HexCer species with d18:1/24:1, d18:1/16:0, and d18:1/12:0 were monitored by the following MRM pairs: Q1/Q3 = 810.6/264.4, 700.6/264.4, and 644.6/264.4, respectively, using product ions of the dehydration sphingolipid base at *m/z* 264.4 [36,37]. On ZIC-HILIC (Fig. 1A), glucose-featuring HexCer species were eluted after their corresponding galactose analogs, mutually separating GlcCer and GalCer species. Phosphatidyl hexosides exhibited the same carbohydrate-dependent elution pattern (Fig. 1B, Fig. S2), as indicated by their respective retention factors for PtdGlc *sn* = 1.2 18:0/20:0 (k = 3.38) and PtdGal 18:0/20:0 (k = 3.36). The preferential retention of glucosylated lipids compared with their galactosylated analogs was also observed on a sulfobetaine stationary phase (Fig. S3). By contrast, on an unmodified silica gel HILIC stationary phase, galactosylated glycolipids were preferentially retained, as indicated by the respective retention factors for PtdGlc (k = 2.90) compared with PtdGal (k = 3.00). Taken together, the preferential retention of glucosylated compared with galactosylated glycolipids appears to be due to the hydrophilic interactions that occur with increased thickness of the hydration layer of the stationary phase [38].

The effect of the fatty acid chain pattern on the retention times was strikingly similar in all columns used. In general, increasing the fatty acyl chain length weakened analyte retention and resulted in reduced retention times. For example, both GlcCer and GalCer featuring a d18:1/12:0 ceramide moiety were eluted later than their d18:1/24:1 ceramide-featuring analogs. By contrast, alteration of the stereoconfiguration of the glycerol moiety gave almost identical retention factors (Fig. 1B). Acetylated PtdGlc (k = 3.16) (i.e., 6-O-acetylation) was weakly retained on the column and therefore eluted earlier than that of non-acetylated PtdGlc. Inositides, such as PtdIns (k = 3.61) and lyso-PtdIns (k = 4.51), were eluted later than their respective glucoside and galactoside analogs in all employed systems. Together, these results correspond well to our previously reported observations using normal phase chromatography [33].

3.3. Analysis of hexosylceramides in brain tissue

To demonstrate the applicability of our ZIC-HILIC method over a broad range of biologically relevant concentrations, the monohexosylceramide content present in total lipid extracts from whole mouse brain tissue at postnatal day 5 (P5) and adult 10-week-old mice was quantified. In contrast to the large amount of GalCer present in adult mouse brain, P5 mouse brain tissue contains only a small amount [39]. The integrity of our brain samples was confirmed with a boric acid-impregnated TLC plate and co-migration with standards. As expected, low amounts of HexCers were found in P5 mouse brain tissue, and GalCer was predominantly found in adult mouse brain (Fig. 2A). The MRM profiles (Fig. 2B, GlcCer species indicated by asterisks) demonstrated that regardless of the large amount of GalCer, GlcCer was still well resolved.

The major fatty acid present in GlcCer from P5 mouse brain was stearic acid (Fig. 2B, P5, light green, d18:1/18:0), whereas the predominant fatty acid in GalCer from adult mouse brain was a nervonic acid residue (d18:1/24:1). In adult mouse brain, the preference for long chain fatty acids of GalCer is preserved. GalCer featuring α-hydroxylated (αOHFA) long chain fatty acids exhibited a longer retention time compared to their non-hydroxylated (non-OHFA) analogs. αOHFAs are characteristically present in

Table 1
Reproducibility of method for brain GlcCer.

	m/z	ZIC-HILIC		HILIC with unmodified silica gel column	
		Contents (fmol/mg lyophilized tissue)	RSD values (%)	Contents (fmol/mg lyophilized tissue)	RSD values (%)
GlcCer(d18:1/16:0)	700.6	0.54	35.6	0.70	42.3
GlcCer(d18:1/18:0)	728.6	38.22	7.2	39.32	7.3
GlcCer(d18:1/20:0)	756.6	2.11	18.5	2.94	19.5
GlcCer(d18:1/22:0)	784.6	3.66	22.1	3.73	21.6
GlcCer(d18:1/24:0)	812.6	4.77	6.3	4.88	6.5
GlcCer(d18:1/24:1)	810.6	15.55	34.5	16.22	26.3

The data were collected from four experiments.

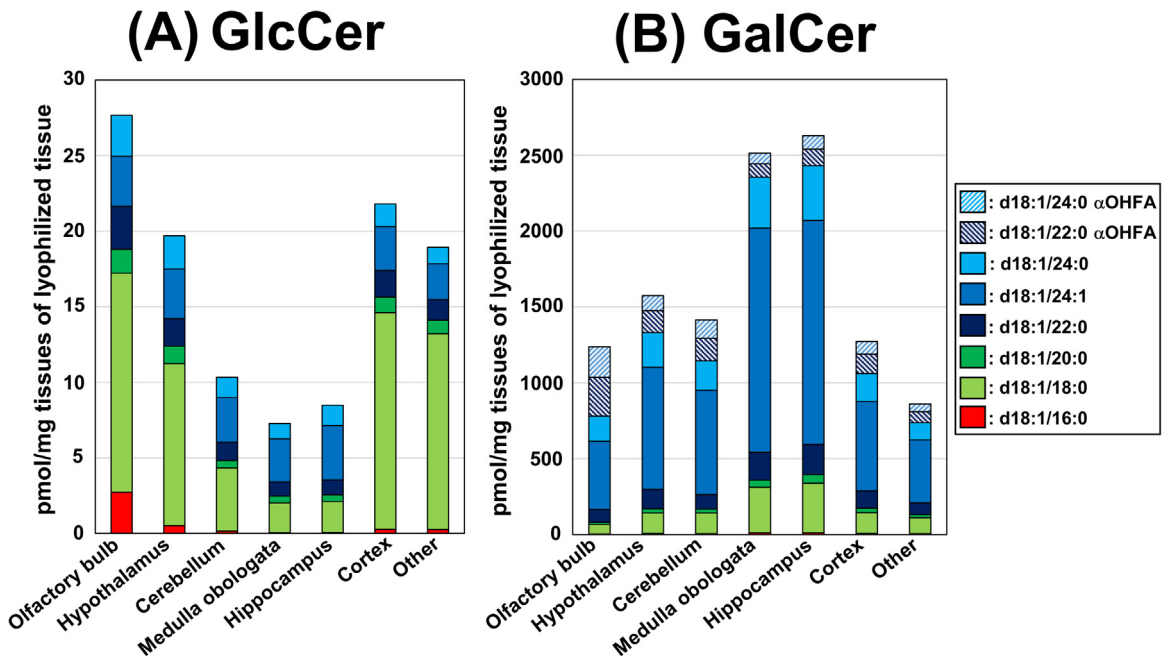

Fig. 3. (A) GlcCer content and (B) GalCer content in different regions of mouse brain. Filled bars in A and B indicate GlcCer and GalCer with non-hydroxy fatty acid (non-OHFA), and striped bars in B indicate GalCer with αOHFA. The content and variability for each compound are shown in Table S2.

GalCer species, which is the predominant constituent in adult mouse brain.

To evaluate the reproducibility of our HILIC methods, the HexCer species, extracted from 9-month-old mouse brains (Table 1), were repeatedly analyzed. An unnatural GlcCer (d18:1/12:0) was added to validate the feasibility of the extraction method. Its recovery was also appropriately 93.8 ± 13.4% (n = 4). Across four samples the relative standard deviations (RSD) on ZIC-HILIC were reproducible, with a range of 6.3% to 35.6%. The unmodified silica gel HILIC RSDs were within 6.5% to 42.3%. In both cases, the determined concentration of low abundant constituents, such as GlcCer (d18:1/16:0), GlcCer (d18:1/20:0), and GlcCer (d18:1/22:0), was comparable, although their respective RSDs were relatively high. Taken together, these results demonstrate that our method is sufficiently robust for the quantification of GlcCer in biological samples, such as brain tissue.

3.4. Distribution of HexCer in brain

Imaging mass spectrometry is a powerful tool for determining the spatial distribution of lipids in the brain [40]. Because of the isobaric nature of HexCer, this technique is incapable of discriminating between different carbohydrate moieties, thus precluding the analysis of minor GlcCer species [41]. Using our ZIC-HILIC method, the concentrations of 14 species of HexCer were determined in seven different regions of adult mouse brain: olfactory bulb, hypothalamus, cerebellum, medulla oblongata, hippocampus, cortex, and other regions (Fig. 3 and Table S2). In each region, the total amount of GalCer exceeded GlcCer. The medulla oblongata and hippocampus were especially rich in GalCer, but poor in GlcCer. In contrast, olfactory bulb, hypothalamus, cortex, and other regions exhibited the highest GlcCer content, but the lowest GalCer content. Thus, the distribution of GlcCer compared to GalCer in brain regions exhibited an inverse relationship, rationalizing the variation of GalCer excess (between 50- and 350-fold) compared to GlcCer.

In terms of fatty acid modification of the ceramide moiety, sizeable amounts of palmitic acid (16:0) were detected in the GlcCer fraction isolated from the olfactory bulb (Fig. 3: red). Stearic acid (18:0) was the main fatty acid found in the four GlcCer-rich regions (Fig. 3: light green). By contrast, the highest content of stearic acid (18:0)-featuring GalCer was in the medulla oblongata and hippocampus, coinciding with the lowest content of stearic acid (18:0)-featuring modified GlcCer. A similar inverse pattern was observed for arachidic acid (20:0), behenic acid (22:0), and lignoceric acid (24:0), despite their relatively low content in GlcCer and GalCer. Nervonic acid (24:1) is the major fatty acid modification found in GalCer, which is specifically enriched in the medulla oblongata and hippocampus (Fig. 3: blue). In the case of GlcCer, nervonic acid-featuring species were distributed evenly. α-Hydroxy fatty acids were found only in the GalCer fraction, with the highest content in the olfactory bulb.

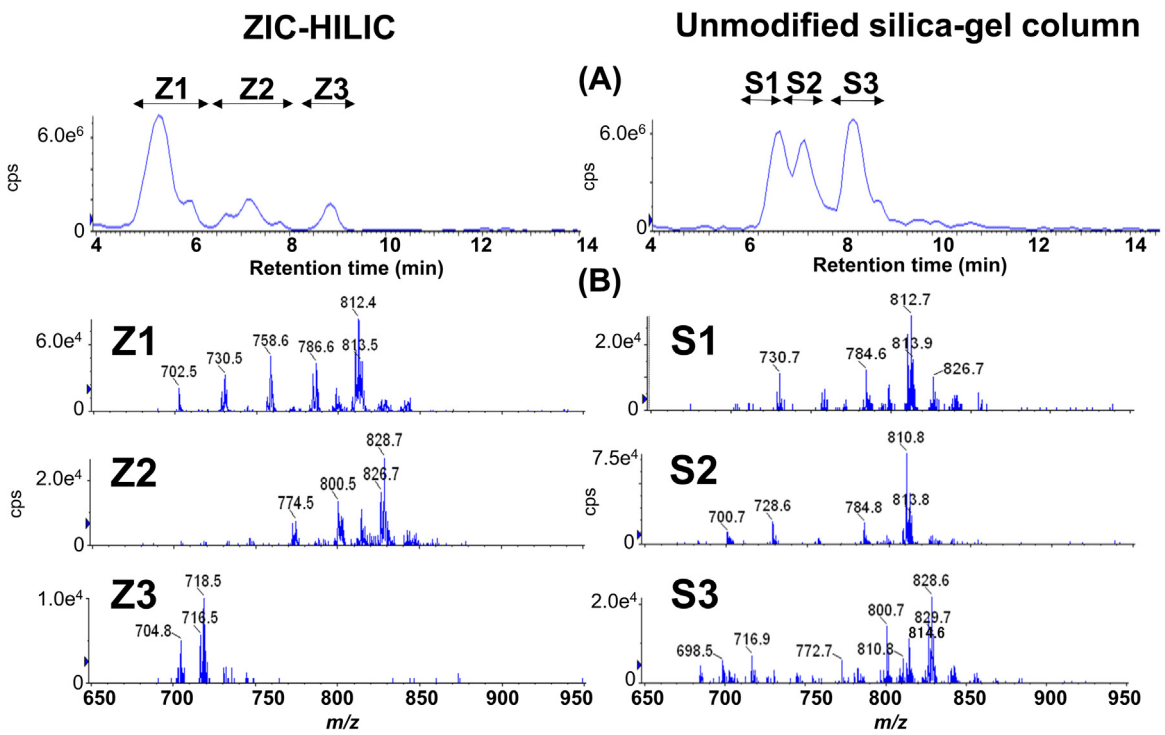

Fig. 4. HILIC-ESI–MS/MS of lipid mixtures extracted from mouse epidermis. (A) Extracted ion chromatograms generated by a neutral-loss scan. Detected peaks were divided into three classes based on retention times (ZIC-HILIC: Z1, Z2, and Z3; unmodified silica gel column: S1, S2, and S3). (B) Mass spectra eluted around each group. Class S3 was separated into two peaks on ZIC-HILIC (Z2: GlcCer species with HFA; Z3: GlcCer species with a trihydroxy sphingoid base).

This heterogeneous distribution of HexCer species likely is related to their region-specific function. For example, a substantial part of white matter is composed of myelin sheath tissue that is rich in nervonic acid-featuring GalCer [42,43]. Consequently, the high content of GalCer with nervonic acid species in the medulla oblongata and hippocampus correlate well with the high content of white matter in these regions of the brain. Therefore, the distinct HexCer composition of each analyzed brain region and the considerable fluctuation of their respective regional content highlights the importance of quantifying local alterations in HexCer composition at the onset and during the progression of neurodegenerative diseases, such as Parkinson disease. If slight differences in GlcCer levels need to be measured further during disease progression, samples should also be analyzed with the HILIC-ESI–MS/MS method combined with an ion-mobility system, which we are currently developing. Taken together, our ZIC-HILIC method is exceptionally suitable for analyzing significant differences in minor GlcCer content across different brain regions.

3.5. Qualitative analysis of hexosylceramide in skin

In general, the epidermis is composed of a complex mixture of hexosylceramides, with a considerable diversity in their ceramide moiety. This includes the presence of an additional hydroxyl group at the α- or ω-position of the fatty acid residue, or at the long chain base, sphingoid base moieties such as 4-hydroxysphinganine or 6-hydroxysphingosine [11,12]. By contrast, the carbohydrate moiety lacks diversity, as it is limited primarily to glucose [44]. Consequently, characterization of the HexCer mixture in mouse epidermis samples is ideal for demonstrating the versatility of our method to discriminate compounds based on differences in their ceramide moiety. To assess the complexity of the ceramide moieties, we detected and characterized HexCers based on LC retention times and *m*/*z* values by neutral loss scan. The neutral loss of 180 Da has been previously associated with the loss of a hexosyl residue by cleavage of its glycosidic linkage [34].

Three distinct classes (Z1, Z2 and Z3) of HexCers were clearly separated by our ZIC-HILIC method based on differences in their ceramide moiety (Fig. 4A). Class Z1 seemed to lack any additional hydroxylation, but did possess a variety of fatty acid residues between C16:0 to C24:1 (Fig. 4B; ZIC-HILIC and Table 2). Class Z2 and Z3 were exclusively composed of HexCer, with an additional hydroxyl group. The ~2 min shift in the retention time of class Z2 compared with class Z1 and the observed *m*/*z* values were indicative of an additional hydroxyl group at either the α- or ω-position of the fatty acid residue (HFA: αOHFA or ωOHFA). By contrast, *m*/*z* values of class Z3 corresponded to known sphingolipids with a trihydroxy long chain base, such as 4-hydroxy-sphinganine and 6-hydroxy-sphingosine [12,45].

For comparison, we used an unmodified silica gel HILIC column to analyze the epidermal HexCer mixture (Fig. 4A). This method resolved classes S1 and S2, which correspond to non-hydroxylated HexCer, and class S3, which corresponds to a mixture of fatty acids and long chain base hydroxylated HexCer. Interestingly, the ions present in class S1 were predominantly 2 Da heavier than the ions present in class S2, indicating a higher degree of saturation in the long chain base moiety. For example, the *m*/*z* value at 812 in S1 and at 810 in S2 corresponded to GlcCer (d18:0/24:1) and GlcCer (d18:1/24:1), respectively. Thus, the method using an unmodified silica gel column was capable of discriminating between GlcCer species with sphingosine (S2) and those with sphinganine (S1). However, the full characterization of unidentified signals, such as *m*/*z* 798.7 and *m*/*z* 810.7, will require additional experiments (Fig. 4A, Table 2). Additionally, minor components such as GlcCer containing αOHFA and trihydroxy sphingoid bases should be characterized. Currently, we are also developing a two-dimensional HILIC-MS method combined with a reversed-phase mode to efficiently characterize minor GlcCer species. These results

Table 2
Structure of mouse epidermal GlcCer.

Peak numbers		*m/z*	Ceramide moieties	
ZIC-HILIC	Unmodified silica-gel		Sphingoid base	Fatty acid
	S2	700.7	d18:1	C16:0
Z1		702.6	d18:0	C16:0
Z1	S2	728.6	d18:1	C18:0
Z1	S1	730.6	d18:0	C18:0
Z1	S1	758.6	d18:0	C20:0
Z1	S2	784.6	d18:1	C22:0
Z1	S1	786.6	d18:0	C22:0
Z1	S1, S2	810.7	d18:1	C24:1
Z1	S2	812.7	d18:1	C24:0
Z1	S1	812.7	d18:0	C24:1
Z1	S1	814.6	d18:0	C24:0
Z2	S3	774.6	d18:1	C20:0 with HFA
Z2	S3	800.6	d18:1	C22:0 with HFA
Z2	S3	814.6	d18:1	C23:0 with HFA
Z2	S3	828.7	d18:1	C24:0 with HFA
Z2	S3	826.7	d18:1	C24:1 with HFA
Z3	S3	716.5	t18:1	C16:0
Z3		718.5	t18:0	C16:0

HFA indicates a mixture of omega/alpha hydroxy fatty acids (ωOHFA and αOHFA).
d18:0 and d18:1: GlcCer featuring dihydroxy sphingolipid bases. t18:0 and t18:1: GlcCer featuring trihydroxy sphingolipid bases.

demonstrate the alternative resolving power of ZIC-HILIC compared with unmodified silica gel HILIC columns.

4. Conclusions

We established and validated the reproducibility of a novel ZIC-HILIC-based HPLC–MS/MS method for the analysis of glycosphingolipids and glycophospholipids. The preferred retention of Ins > Glc > Gal allowed the outright identification of the carbohydrate moiety despite their isobaric nature. Additionally, GlcCer, the minor component in brain samples, was confidently analyzed, even in the presence of a 350 times excess of GalCer. In skin samples, our ZIC-HILIC method demonstrated its potential to resolve fatty acid and long chain base hydroxylation. Comparison of our new method with an unmodified silica gel HILIC column revealed an inverted retention profile and separation characteristics with respect to the lipid moiety. Thus, our approach with two HILIC methods successfully quantified glucosylated lipids in brain and skin tissues.

Acknowledgments

We thank Dr. Sumiko Hamanaka (Josai University) for providing the samples of lipid mixtures extracted from the epidermis. We also thank Dr. Shota Sakai (Hokkaido University) for valuable suggestions prior to submission. This work was supported by Grant-in-Aid for B, 15K19016 (K.N.) from the Ministry of Education, Culture, Sports, Science and Technology of Japan.

Appendix A. Supplementary data

Supplementary data associated with this article can be found, in the online version, at http://dx.doi.org/10.1016/j.jchromb.2016.07.047.

References

[1] Y. Ishibashi, A. Kohyama-Koganeya, Y. Hirabayashi, New insights on glucosylated lipids: metabolism and functions, Biochim. Biophys. Acta 1831 (2013) 1475–1485.
[2] Y. Hirabayashi, A world of sphingolipids and glycolipids in the brain–novel functions of simple lipids modified with glucose, Proc. Jpn. Acad. Ser. B: Phys. Biol. Sci. 88 (2012) 129–142.
[3] S. Kunimoto, T. Kobayashi, S. Kobayashi, K. Murakami-Murofushi, Expression of cholesteryl glucoside by heat shock in human fibroblasts, Cell Stress Chaperones 1 (2000) 3–7.
[4] H. Akiyama, S. Kobayashi, Y. Hirabayashi, K. Murakami-Murofushi, Cholesterol glucosylation is catalyzed by transglucosylation reaction of β-glucosidase 1, Biochem. Biophys. Res. Commun. 441 (2013) 838–843.
[5] T. Coetzee, N. Fujita, J. Dupree, R. Shi, A. Blight, K. Suzuki, K. Suzuki, B. Popko, Myelination in the absence of galactocerebroside and sulfatide: normal structure with abnormal function and regional instability, Cell 86 (1996) 209–219.
[6] S. Watanabe, S. Endo, E. Oshima, T. Hoshi, H. Higashi, K. Yamada, K. Tohyama, T. Yamashita, Y. Hirabayashi, Glycosphingolipid synthesis in cerebellar Purkinje neurons: roles in myelin formation and axonal homeostasis, Glia 58 (2010) 1197–1207.
[7] A. Schwarz, A.H. Futerman, Distinct roles for ceramide and glucosylceramide at different stages of neuronal growth, J. Neurosci. 17 (1997) 2929–2938.
[8] Y. Nagatsuka, T. Kasama, Y. Ohashi, J. Uzawa, Y. Ono, K. Shimizu, Y. Hirabayashi, A new phosphoglycerolipid 'phosphatidylglucose', found in human cord red cells by multi-reactive monoclonal anti-i cold agglutinin, mAb GL-1/GL-2, FEBS Lett. 497 (2001) 141–147.
[9] A.T. Guy, Y. Nagatsuka, N. Ooashi, M. Inoue, A. Nakata, P. Greimel, A. Inoue, T. Nabetani, A. Murayama, K. Ohta, Y. Ito, J. Aoki, Y. Hirabayashi, H. Kamiguchi, NEURONAL DEVELOPMENT. Glycerophospholipid regulation of modality-specific sensory axon guidance in the spinal cord, Science 349 (2015) 974–977.
[10] Y.A. Hannun, L.M. Obeid, Many ceramides, J. Biol. Chem. 286 (2011) 27855–27862.
[11] M. Abe, E. Ohima, S. Sakai, Y. Hirabayashi, T. Tsuchida, S. Hamanaka, Sphingolipids of the murine hair, J. Soc. Jap. Woman Sci. 12 (2012) 32–43.
[12] S. Hamanaka, M. Hara, H. Nishio, F. Otsuka, A. Suzuki, Y. Uchida, Human epidermal glucosylceramides are major precursors of stratum corneum ceramides, J. Invest. Dermatol. 119 (2002) 416–423.
[13] X. Han, K. Yang, R.W. Gross, Multi-dimensional mass spectrometry-based shotgun lipidomics and novel strategies for lipidomic analyses, Mass Spectrom. Rev. 31 (2012) 134–178.
[14] T. Alvarez-Segura, C. Ortiz-Bolsico, J.R. Torres-Lapasió, M.C. García-Álvarez-Coque, Serial versus parallel columns using isocratic elution: a comparison of multi-column approaches in mono-dimensional liquid chromatography, J. Chromatogr. A 1390 (2015) 95–102.
[15] Y. Hirabayashi, A. Hamanaka, M. Matsumoto, K. Nishimura, An improved method for the separation of molecular species of cerebrosides, Lipids 21 (1986) 710–714.
[16] C. Zhu, A. Dane, G. Spijksma, M. Wang, J. van der Greef, G. Luo, T. Hankemeier, R.J. Vreeken, An efficient hydrophilic interaction liquid chromatography separation of 7 phospholipid classes based on a diol column, J. Chromatogr. A 1220 (2012) 26–34.
[17] M. Schwalbe-Herrmann, J. Willmann, D.K. Leibfritz, Separation of phospholipid classes by hydrophilic interaction chromatography detected by electrospray ionization mass spectrometry, J. Chromatogr. A 1217 (2010) 5179–5183.
[18] Y. Okazaki, Y. Kamide, M. Yokota-Hirai, K. Saito, Plant lipidomics based on hydrophilic interaction chromatography coupled to ion trap time-of-flight mass spectrometry, Metabolomics 9 (2013) S121–131.
[19] P. Jandera, Stationary and mobile phases in hydrophilic interaction chromatography: a review, Anal. Chim. Acta 692 (2011) 1–25.

[20] N.P. Dinh, T. Jonsson, K. Irgum, Water uptake on polar stationary phases under conditions for hydrophilic interaction chromatography and its relation to solute retention, J. Chromatogr. A 1320 (2013) 33–47.
[21] R.L. Shaner, J.C. Allegood, H. Park, E. Wang, S. Kelly, C.A. Haynes, M.C. Sullards, A.H. Merrill Jr., Quantitative analysis of sphingolipids for lipidomics using triple quadrupole and quadrupole linear ion trap mass spectrometers, J. Lipid Res. 50 (2009) 1692–1707.
[22] N. Brignol, K. Chang, R. Hamler, A.E. Schilling, R. Khanna, D.J. Lockhart, S.W. Clark, E.R. Benjamin, Mol. Genet. Metab. 105 (2012) S22.
[23] J. Snider, Simultaneous Quantitative Analysis of Glucosylceramide and Galactosylceramide Species by Supercritical Fluid Chromatography Tandem Mass Spectrometry, Medical University of South Carolina Waring Historical Library Department of Biochemistry and Molecular Biology, 2011.
[24] M. Boutin, Y. Sun, J.J. Shacka, C. Auray-Blais, Tandem mass spectrometry multiplex analysis of glucosylceramide and galactosylceramide isoforms in brain tissues at different stages of Parkinson disease, Anal. Chem. 88 (2016) 1856–1863.
[25] L. Zheng, R. T'Kind, S. Decuypere, S.J. von Freyend, G.H. Coombs, D.G. Watson, Profiling of lipids in *Leishmania donovani* using hydrophilic interaction chromatography in combination with Fourier transform mass spectrometry, Rapid Commun. Mass Spectrom. 24 (2010) 2074–2082.
[26] G. Greco, S. Grosse, T. Letzel, Study of the retention behavior in zwitterionic hydrophilic interaction chromatography of isomeric hydroxy- and aminobenzoic acids, J. Chromatogr. A 1235 (2012) 60–67.
[27] R.I. Chirita, C. West, S. Zubrzycki, A.L. Finaru, C. Elfakir, Investigations on the chromatographic behaviour of zwitterionic stationary phases used in hydrophilic interaction chromatography, J. Chromatogr. A 1218 (2011) 5939–5963.
[28] T. Ito, E.E. Herter, J. Baidoo, M.E. Lao, A.M. Vega-Sánchez, P.D. Smith-Moritz, J.D. Adams, B. Keasling, C.J. Usadel, J.L. Petzold, J.L. Heazlewoodd, Analysis of plant nucleotide sugars by hydrophilic interaction liquid chromatography and tandem mass spectrometry, Anal. Biochem. 448 (2014) 14–22.
[29] Y. Takegawa, K. Deguchi, T. Keira, H. Ito, H. Nakagawa, S.I. Nishimura, Separation of isomeric 2-aminopyridine derivatized N-glycans and N-glycopeptides of human serum immunoglobulin G by using a zwitterionic type of hydrophilic-interaction chromatography, J. Chromatogr. A 1113 (2006) 177–181.
[30] P. Greimel, M. Lapeyre, Y. Nagatsuka, Y. Hirabayashi, Y. Ito, Syntheses of phosphatidyl-beta-D-glucoside analogues to probe antigen selectivity of monoclonal antibody 'DIM21', Bioorg. Med. Chem. 16 (2008) 7210–7217.
[31] Y. Nagatsuka, Y. Horibata, Y. Yamazaki, M. Kinoshita, Y. Shinoda, T. Hashikawa, H. Koshino, T. Nakamura, Y. Hirabayashi, Phosphatidylglucoside exists as a single molecular species with saturated fatty acyl chains in developing astroglial membranes, Biochemistry 45 (2006) 8742–8750.
[32] E.G. Bligh, W.J. Dyer, Can. J. Biochem. Physiol. 37 (1959) 911–917.
[33] S. Ito, T. Nabetani, Y. Shinoda, Y. Nagatsuka, Y. Hirabayashi, Quantitative analysis of a novel glucosylated phospholipid by liquid chromatography-mass spectrometry, Anal. Biochem. 376 (2008) 252–257.
[34] K. Nakajima, A. Kohyama-Koganeya, Y. Hirabayashi, Profiling of glycosylceramides by liquid-chromatography-tandem mass spectrometry, Glycosci.: Biolo. Med. (2014) 103–111.
[35] E.L. Kean, Separation of gluco- and galactocerebrosides by means of borate thin-layer chromatography, J. Lipid Res. 7 (1966) 449–452.
[36] C.E. Costello, J.E. Vath, Tandem mass spectrometry of glycolipids, Methods Enzymol. 193 (1988) 738–768.
[37] B. Domon, C.E. Costello, Structure elucidation of glycosphingolipids and gangliosides using high-performance tandem mass spectrometry, Biochemistry 27 (1988) 1534–1543.
[38] W. Kamichatani, Y. Inoue, A. Yamamoto, Separation properties of saccharides on a hydrophilic stationary phase having hydration layer formed zwitterionic copolymer, Anal. Chim. Acta 853 (2015) 602–607.
[39] S. Ngamukote, M. Yanagisawa, T. Ariga, S. Ando, R.K. Yu, Developmental changes of glycosphingolipids and expression of glycogenes in mouse brains, J. Neurochem. 103 (2007) 2327–2341.
[40] Y. Sugiura, M. Setou, Imaging mass spectrometry for visualization of drug and endogenous metabolite distribution: toward in situ pharmacometabolomes, J. Neuroimmune Pharmacol. 5 (2010) 31–43.
[41] M.F. Snel, M. Fuller, High-spatial resolution matrix-assisted laser desorption ionization imaging analysis of glucosylceramide in spleen sections from a mouse model of Gaucher disease, Anal. Chem. 82 (2010) 3664–3670.
[42] S. Cha, E.S. Yeung, Colloidal graphite-assisted laser desorption/ionization mass spectrometry and MS_n of small molecules 1. Imaging of cerebrosides directly from rat brain tissue, Anal. Chem. 79 (2007) 2373–2385.
[43] S.C. Zhang, Defining glial cells during CNS development, Nat. Rev. Neurosci. 2 (2001) 840–842.
[44] S. Hamanaka, T. Yamamoto, C. Asagami, Occurrence of galactosylceramide in pig epidermal cells, Biochim. Biophys. Acta 961 (1988) 374–377.
[45] R.J. Robson, M.E. Stewartm, S. Michelsen, N.D. Lazo, D.T. Downing, 6-Hydroxy-4-sphingenine in human epidermal ceramides, J. Lipid Res. 35 (1994) 2060–2068.